Open access • Journal Article • DOI:10.1364/OL.20.002457

Fabrication, modeling, and characterization of form-birefringent nanostructures.

Fang Xu, Rong-Chung Tyan, Pang-Chen Sun, Yeshayahu Fainman ...+2 more authors

Institutions: University of California, San Diego, California Institute of Technology

Published on: 15 Dec 1995 - Optics Letters (Optical Society of America)

Topics: Birefringence, Rigorous coupled-wave analysis, Nanostructure, Electron-beam lithography and Refractive index

Fabrication, modeling, and characterization of form-birefringent nanostructures

Fang Xu, Rong-Chung Tyan, Pang-Chen Sun, and Yeshayahu Fainman

Department of Electrical and Computer Engineering, University of California, San Diego, La Jolla, California 92037

Chuan-Cheng Cheng and Axel Scherer

Department of Electrical Engineering, California Institute of Technology, Pasadena, California 91125

Received August 15, 1995

A 490-nm-deep nanostructure with a period of 200 nm was fabricated in a GaAs substrate by use of electron-beam lithography and dry-etching techniques. The form birefringence of this microstructure was studied numerically with rigorous coupled-wave analysis and compared with experimental measurements at a wavelength of 920 nm. The numerically predicted phase retardation of 163.3° was found to be in close agreement with the experimentally measured result of 162.5°, thereby verifying the validity of our numerical modeling. The fabricated microstructures show extremely large artificial anisotropy compared with that available in naturally birefringent materials and are useful for numerous polarization optics applications.

The form-birefringence or artificial-birefringence effect occurs when the period of such microstructures is much less than the wavelength of the incident optical field and the far field of the transmitted radiation will possess only zero-order diffraction. The two prevalent approaches to characterize such artificial dielectric properties of the microstructured boundary use the effective medium theory[1] and rigorous coupled-wave analysis[2,3] (RCWA). In this study we choose to use RCWA because the simpler effective medium theory does not provide accurate results when the microstructured grating period approaches the wavelength of the radiation.[3,4] Form-birefringent nanostructures (FBN's) have several unique properties[3] that make them superior to naturally birefringent materials: (i) A high value for the strength of form birefringence, $\Delta n/n$, can be obtained by the selection of substrate dielectric materials with a large refractive-index difference (here Δn and n are the difference and the average effective indices of refraction, respectively, for the two orthogonal polarizations); for example, a high-spatial-frequency surface-relief grating of rectangular profile on a GaAs substrate provides a $\Delta n/n$ value of $\sim$0.63, which is much larger than those found for naturally birefringent materials (e.g., for calcite the value of $\Delta n/n$ is $\sim$0.1). (ii) The magnitude of form birefringence, Δn, can be adjusted by variation of the duty ratio as well as of the shape of the microstructures.[3] (iii) FBN's can be used to modify the reflection properties of the dielectric boundaries.[3,5] Such FBN's are useful for constructing polarization-selective beam splitters[6,7] and general-purpose polarization-selective diffractive optical elements such as birefringent computer-generated holograms[8] (BCGH's).

A BCGH is a general-purpose diffractive optical element that has two independent though arbitrary impulse responses for the two orthogonal linear polarizations. BCGH elements are useful in various applications.[8] In its original design[9] a BCGH consists of two surface-relief substrates with at least one of them birefringent. The two independent etch depths of the BCGH element provide the two degrees of freedom necessary to encode the two independent phase functions. However, the BCGH fabrication process can be simplified by use of a single FBN made of an isotropic substrate. One can obtain the two degrees of freedom necessary for construction of a BCGH by varying, for example, the duty ratio and the etch depth of the dielectric nanostructures. In this Letter we investigate the fabrication and characterization of FBN's to determine their usefulness for construction of a form-birefringent computer-generated hologram.

Fabrication of FBN's for visible and near-infrared wavelength regions is a challenging task. In the past, artificial birefringence was observed experimentally for microstructures with a relatively large period that can be operated in the microwave or far-infrared spectrum range.[5] For visible and near-infrared radiation-range applications the artificial dielectrics were fabricated with a stratified multilayer structure[10] or by the recording of interference patterns of two coherent light beams to create a subwavelength grating in a photoresist.[11] Neither method is suitable for our BCGH applications since the former creates the form birefringence in a direction perpendicular to the substrate surface and the latter does not provide design flexibility in terms of microstructure shape and the values of the dielectric constants. To achieve the design and the fabrication flexibility required by a BCGH, we use electron-beam lithography to generate the high-spatial-frequency patterns.

The fabrication procedures of FBN's in GaAs substrates are shown schematically in Fig. 1. First, a GaAs substrate was coated with a layer of SiO_2, then a layer of Au, and finally a layer of high-molecular-weight poly(methyl methacrylate) (PMMA). Electron-beam lithography with a 30-kV

0146-9592/95/242457-03$6.00/0

incident beam energy was used to define the high-resolution linear gratings over a square area of 100 μm $\times$ 100 μm on the spun-on 70-nm-thick resist layer. The PMMA pattern was developed for 14 s in a 3:7 mixture of $C_2H_5OCH_7CH_2OH$ in CH_3OH and then was transferred onto the 70-nm-thick Au layer by ion milling with 1500-V Ar ions. This Au layer was used as a dry-etching mask to transfer the patterns into the 100-nm-thick layer of sputter-deposited SiO_2 by reactive-ion etching. During this etching process, 60-mTorr C_2F_4 was used as the reactive gas, and a 300-V bias voltage was applied (50 W of rf power) at an etch rate of 20 nm/min. Then, a chemically assisted ion-beam etching system helped to etch the high-resolution nanostructure to the desired depth in the GaAs by using an Ar-ion beam assisted with Cl_2 reactive gas. Finally, we removed the SiO_2 mask by immersing the sample into buffered HF. The 490-nm-deep nanostructure with a period of 200 nm fabricated in GaAs substrate was inspected under a scanning-electron microscope (SEM). The top view and the cross-sectional view of the fabricated nanostructure are shown in Figs. 2(a) and 2(b), respectively.

The experimental setup for characterization of the form birefringence of fabricated nanostructures is shown schematically in Fig. 3. An Ar^+-pumped Ti:sapphire laser was operated at a wavelength of 920 nm, where the GaAs substrate is transparent with minimum absorption. The polarization of the laser beam was controlled by a polarization rotator so that the normally incident optical wave was polarized linearly at 45° with respect to the grooves' direction. We used a microscope objective to focus the incident beam onto the 100 μm $\times$ 100 μm microstructure pattern. At a distance of 1 m from the sample we inserted a 1-cm-diameter aperture stop and a polarization analyzer followed by a photodetector. The aperture stop was introduced to avoid contributions of the obliquely incident light and diffracted field from the edges of the sample, thereby ensuring the validity of the paraxial approximation necessary for our polarization measurements. A Glan–Thompson-type polarizer was used as an output analyzer.

For the experimental characterization of the FBN we used Jones calculus. Let the Jones matrix of the form-birefringent nanostructure on a GaAs substrate be given by

$$J_s = \begin{bmatrix} a & 0 \\ 0 & b\exp(j\phi_s) \end{bmatrix}, \tag{1}$$

where a and b are the amplitude transmittances of the horizontally and vertically polarized light (i.e., perpendicular and parallel to the grooves' direction), and ϕ_s is the phase difference between them on propagation through the FBN. The output fields for these two polarizations can be formulated as

$$\begin{bmatrix} E_{H\text{out}} \\ E_{V\text{out}} \end{bmatrix} = \mathbf{J}(\theta)\begin{bmatrix} a & 0 \\ 0 & b\exp(j\phi_s) \end{bmatrix}\begin{bmatrix} 1 \\ 1 \end{bmatrix}\frac{E_i}{\sqrt{2}}, \tag{2}$$

where

$$\mathbf{J}(\theta) = \mathbf{R}(-\theta)\mathbf{J}(0)\mathbf{R}(\theta) = \begin{bmatrix} \cos\theta & \sin\theta \\ -\sin\theta & \cos\theta \end{bmatrix}\begin{bmatrix} 1 & 0 \\ 0 & 0 \end{bmatrix}\begin{bmatrix} \cos\theta & -\sin\theta \\ \sin\theta & \cos\theta \end{bmatrix} \tag{3}$$

represents the Jones matrix of an analyzer that is aligned at an angle θ with respect to the vertical direction, and the input field is 45° linearly polarized. The intensity measured at the detector is given by

$$I_{\text{out}} = (a^2\cos^2\theta + b^2\sin^2\theta + 2ab\sin 2\theta\cos\phi_s)\frac{I_{\text{in}}}{2}. \tag{4}$$

Figure 4 shows a typical curve of measured intensity versus the orientation angle of the analyzer, θ, in the setup of Fig. 3. The two curves correspond to the measurements of the GaAs substrate with and without the FBN. We curve fitted the measured data by using Eq. (4) (see the solid and dashed curves in Fig. 4), which yielded the resultant parameters $a = 0.67$, $b = 0.57$, and $\phi_s = 162.5°$. Note

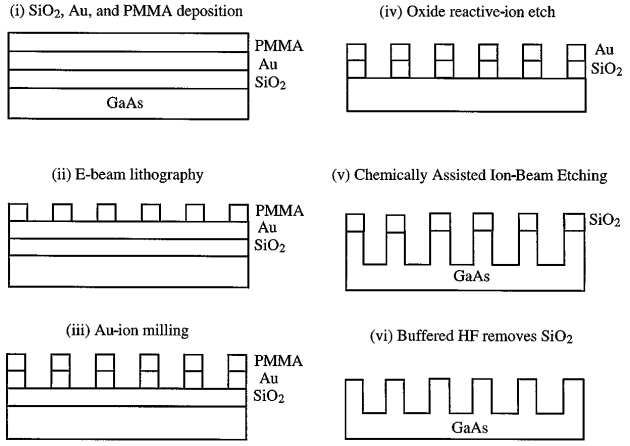

Fig. 1. Schematic of the procedures for the fabrication of form-birefringent nanostructures in GaAs substrates.

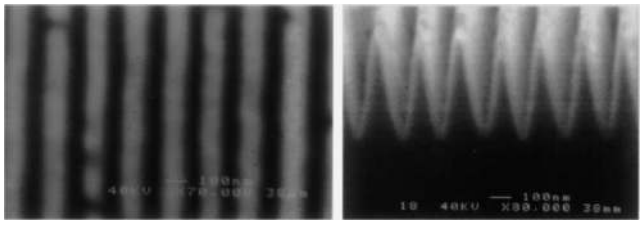

Fig. 2. SEM photographs of the fabricated form-birefringent nanostructure in a GaAs substrate: (a) top and (b) cross-sectional views.

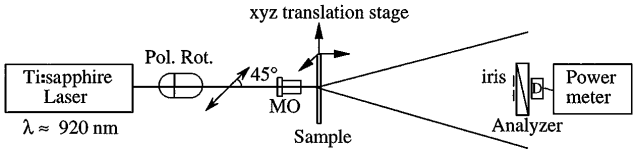

Fig. 3. Schematic of the experimental setup for the characterization of form-birefringent nanostructures. Pol. Rot., polarization rotator; MO, microscope objective.

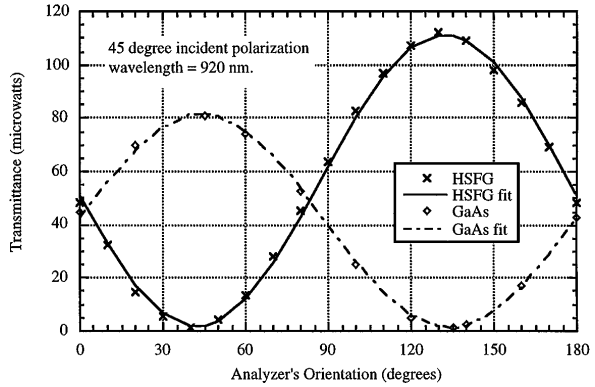

Fig. 4. Experimental measurements and curve-fitted results of the transmitted intensity versus the orientation of the analyzer for a GaAs substrate with and without the form-birefringent high-spatial-frequency grating (HSFG).

that ϕ_s is the positive phase difference between the fields at vertical and horizontal polarizations because the effective index for polarization parallel to the grooves of the nanostructure is larger than that for the perpendicular polarization.[3] From Fig. 4 we can also observe that the transmittance from the GaAs substrate with the FBN is larger than that from the GaAs substrate alone. This effect is obtained because the effective indices of the nanostructure for both polarizations are smaller than those of the GaAs substrate, and therefore the nanostructure pattern acts as an antireflection coating.

The parameters a, b, and ϕ_s were also calculated numerically with RCWA applied to the measured profile [Fig. 2(b)] of the fabricated FBN in GaAs substrate. The profile is described by a trapezoid shape, with its top edge being 5% of the period and the bottom edge being 95% of its period. The period and the depth of the GaAs nanostructure were estimated from the SEM photographs of Fig. 2 to be 200 and 490 nm, respectively. The GaAs substrate is 500 μm thick, with a refractive index of 3.57 and an absorption coefficient of 3.25×10^{-5}, which are interpolated from the data in Ref. 12. The numerical simulations provide parameters $a = 0.743$, $b = 0.714$, and $\phi_s = 163.3°$. The computer-simulation result for the phase difference between the two orthogonal polarizations is found to be in very good agreement (0.5% difference) with the measured results, confirming the validity of our RCWA-based numerical model. We anticipate that the slight difference in the amplitude transmission coefficients occurs as a result of (i) some scattering loss on the surface of the nanostructure, (ii) diffraction scattering on the limiting aperture of the nanostructure, (iii) inaccuracy in the calculated absorption coefficient for the GaAs substrate, and (iv) inaccuracy in the assumed profile and depth.

The characteristics of the fabricated nanostructure shown in Fig. 4 indicate that it will be possible to obtain a relative phase retardation of π (e.g., a half-wave plate) between the vertical and horizontal polarizations. Note that, by rotating the orientation of the periodic nanostructure on the GaAs substrate by 90°, we will obtain the negative value $-\pi$ for the phase retardation between the vertical and horizontal polarizations. Therefore by controlling the orientation of the periodic nanostructure we will be able to obtain a total range of phase retardation between $-\pi$ and π, which will be sufficient for the design of a binary-phase single-substrate BCGH. Furthermore, this phase-retardation range will be useful for encoding the phase difference of a multiple-phase-level BCGH, whereas absolute relative phase will need to be corrected by mean of other methods.

In conclusion, we have fabricated a 490-nm form-birefringent nanostructure with a period of 200 nm in a GaAs substrate. Form birefringence of the nanostructure was studied numerically with RCWA and compared with experimental measurements at a wavelength of 920 nm. The theoretical modeling used the grating profile measured from SEM photographs of these nanostructures. The predicted phase retardation of 163.3° is found to be in close agreement with the experimentally measured result of 162.5°. Controlling the orientation of the dielectric nanostructure permits us to obtain a phase retardation varying from $-\pi$ to π for the two orthogonal linear polarizations. The fabricated nanostructures show extremely large artificial anisotropy compared with that available in naturally birefringent materials and are useful not only for single-substrate form-birefringent computer-generated holograms[3] but also for numerous other polarization optics applications.

This study was funded by the National Science Foundation, the U.S. Air Force Office for Scientific Research, the Optical Technology Center of the Advanced Research Projects Agency, and the Rome Laboratory.

References

1. S. M. Rytov, Sov. Phys. JETP **2,** 466 (1956).
2. E. N. Glytsis and T. K. Gaylord, Appl. Opt. **31,** 4459 (1992).
3. I. Richter, P. C. Sun, F. Xu, and Y. Fainman, Appl. Opt. **34,** 2421 (1995).
4. H. Kikuta, H. Yoshida, and K. Iwata, Opt. Rev. **2,** 92 (1995).
5. D. H. Raguin and G. M. Morris, Appl. Opt. **32,** 1154 (1993).
6. A. Ohba, Y. Kimura, S. Sugama, Y. Urino, and Y. Ono, Jpn. J. Appl. Phys. Suppl. **28,** 359 (1989).
7. P. Kipfer, M. Collischon, H. Haidner, J. Schwider, N. Streibl, and J. Lindolf, Opt. Eng. **33,** 79 (1994).
8. F. Xu, J. E. Ford, and Y. Fainman, Appl. Opt. **34,** 256 (1995).
9. J. E. Ford, F. Xu, K. Urquhart, and Y. Fainman, Opt. Lett. **18,** 456 (1993).
10. T. Sato, K. Shiraishi, K. Tsuchida, and S. Kawakami, Appl. Phys. Lett. **61,** 2633 (1992).
11. L. H. Cescato, E. Gluch, and N. Streibl, Appl. Opt. **29,** 3286 (1990).
12. E. D. Palik, ed., *Handbook of Optical Constants of Solids* (Academic, New York, 1985).